Submitted to *Geophysical Research Letters*, April 2007

The evolution of the stratopause during the 2006 major warming: Satellite Data and Assimilated Meteorological Analyses

Gloria L. Manney[1,2], Kirstin Krüger[3], Steven Pawson[4], Michael J. Schwartz[1], William H. Daffer[5], Nathaniel J. Livesey[1], Martin G. Mlynczak[6], Ellis E. Remsberg[6], James M. Russell III[7], and Joe W. Waters[1]

Abstract. Microwave Limb Sounder and Sounding of the Atmosphere with Broadband Emission Radiometry data show the polar stratopause, usually higher than and separated from that at midlatitudes, dropping from ∼55–60 to near 30 km during the development of a major stratospheric sudden warming (SSW) in January 2006; the stratopause and mesosphere subsequently cool dramatically during and following the peak of the SSW. After a period when the stratosphere is nearly isothermal, a cool stratopause reforms near 75 km in early February, then drops to ∼55 km and warms. The stratopause is separated in longitude as well as latitude, with lowest temperatures in the transition regions between higher and lower stratopauses. Operational assimilated meteorological analyses, which are not constrained by data at stratopause altitude, do not capture a secondary temperature maximum that overlies the stratopause or the very high stratopause that reforms after the SSW; they underestimate the stratopause altitude variation during the SSW. High-quality daily satellite temperature measurements are invaluable in improving our understanding of stratopause evolution and its representation in models and assimilation systems.

1. Introduction

The stratopause region has not been extensively studied, largely because of the sparsity and poor resolution of data covering the upper stratosphere/lower mesosphere (USLM). *Labitzke* [1972] used rocket and early satellite data to show a drop of ∼20 km in stratopause altitude during a stratospheric sudden warming (SSW), accompanied by a mesospheric cooling that was analyzed using radiation calculations. *Hitchman et al.* [1989] showed that the elevated "separated" polar winter stratopause was consistent with formation via gravity wave (GW) processes. Until the past several years, global daily temperature measurements covering the USLM were available for only a few short periods and/or had extremely poor (∼15 km or greater) vertical resolution. Since the launch of the Sounding of the Atmosphere with Broadband Emission Radiometry (SABER) instrument in January 2002, such profiles have been available with good quality and resolution [∼2 km, e.g., *Remsberg et al.*, 2003] and ∼3° along-orbit spacing, but with an ∼60-day "yaw" cycle whereby the instrument only observes high latitudes in one hemisphere at a time. Since August 2004, the Microwave Limb Sounder (MLS) on NASA's Earth Observing System Aura satellite has provided daily near-global (±82°) temperature profiles from 315 to 0.001 hPa with vertical resolution of ∼6–9 km in the USLM and ∼1.6° along-orbit spacing [e.g., *Livesey et al.*, 2005; *Waters et al.*, 2006].

Operational assimilated meteorological analyses, including ones that extend through the USLM from NASA's Global

[1]Jet Propulsion Laboratory, California Institute of Technology, Pasadena, CA, USA.
[2]Also at New Mexico Institute of Mining and Technology, Socorro, New Mexico, USA
[3]Leibniz-Institute for Marine Sciences at Kiel University (IFM-GEOMAR), Kiel, Germany.
[4]NASA Goddard Space Flight Center, Greenbelt, Maryland, USA.
[5]Columbus Technologies and Services Inc, Pasadena, CA, USA.
[6]NASA Langley Research Center, Hampton, Virginia, USA.
[7]Hampton University, Hampton, Virginia, USA.

Modeling and Assimilation Office (GMAO) and the European Center for Medium-Range Weather Forecasts (ECMWF), are often used for studies of middle atmosphere temperature. Currently, the highest altitude temperature inputs to these are radiances from nadir sounding satellites in the upper stratosphere with very poor vertical resolution. USLM temperatures are thus very weakly constrained by data and rely primarily on the underlying general circulation models (GCMs), which have differing treatments of the mesosphere, model top effects, and GW parameterizations. Since data for comparisons have been sparse, the quality of the analyses in the USLM is largely unknown.

The evolution of the stratopause during the prolonged SSW that began in January 2006 is detailed here using MLS (v1.5) and SABER (v1.06) data, and compared with that in GMAO's Goddard Earth Observing System v4.03 and v5.01 (GEOS-4 and GEOS-5) analyses [*Bloom et al.*, 2005; *Reinecker et al.*, 2007] and ECMWF analyses from the T799/91-level system that became operational in February 2006 [*Untch et al.*, 2006]. Both analysis systems use GCMs with a model top at 0.01 hPa. The GEOS analyses use a simple non-orographic GW parameterization [*Garcia and Boville*, 1994] to represent waves with non-zero phase speed that are important in the USLM; ECMWF uses Rayleigh friction at altitudes above 5 hPa to slow down the otherwise too strong polar night jet.

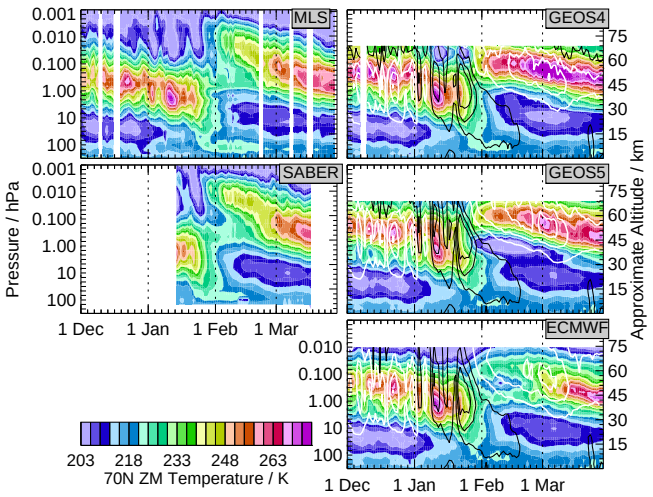

Figure 1. Pressure-time sections at 70°N of zonal mean temperature from (top to bottom) MLS and SABER satellite data, and GEOS-4, GEOS-5, and ECMWF meteorological analyses, from 1 December 2005 through 31 March 2006. Overlaid contours on GEOS and ECMWF plots are 70°N zonal mean winds from -60 to 90 ms^{-1} by 30 ms^{-1}, with negative and zero values in black, positive values in white.

2. Evolution of the Stratopause

Figure 1 shows zonal mean 70°N temperatures and zonal winds during the 2005–2006 northern hemisphere (NH) winter; Figure 2 shows the latitude dependence of stratopause altitude and temperature. Until early January, the polar stratopause altitude was fairly constant near 55–60 km (Figures 1 and 2; the higher stratopause north of ∼60°N until late December (Figure 2) shows the climatological pattern noted by *Hitchman et al.* [1989]. *Hitchman et al.* [1989] found the polar stratopause was warmer than that in midlatitudes; the MLS data show a transition from cooler to warmer in early December. Zonal mean easterlies (black contours on analysis panels) appeared in the USLM in early January, and the conditions for a major SSW were fulfilled by 21 January, with easterlies north of 60°N (not shown) at 10 hPa. Concurrently with the appearance of easterlies in the USLM, the stratopause began dropping and warming rapidly. Stratopause cooling began in mid- to late-January, when easterlies were at a maximum in the USLM and extended through the middle stratosphere; the cooling started just poleward of the reforming westerly jet core. By late January, the stratopause was very low and ill-defined, with a cool, nearly isothermal region from ∼30 to 0.1 hPa. The stratopause reappeared as a well-defined structure in early February near 0.01 hPa (∼75 km) with much lower temperatures than before the SSW. The strong latitudinal gradients in stratopause altitude poleward of the jet core after its reformation show the separation of the polar stratopause from that at midlatitudes. *Siskind et al.* [2007] presented GCM simulations suggesting that the high stratopause in mid-February 2006 resulted from filtering by disturbed stratospheric winds during the SSW of GWs that usually break at and above 50 km; the GW parameterization used was critical to whether or not the model captures the very high stratopause after the warming. In February and early March, the stratopause dropped and warmed, reaching an altitude and temperature similar to those in early winter by mid-March.

Stratopause evolution agrees well between SABER and MLS data; it is warmer and typically slightly lower in MLS v1.5 than in SABER data; MLS v1.5 temperatures have a known high bias with respect to correlative data in the upper stratosphere [e.g., *Froidevaux et al.*, 2006]. Stratopause evolution also agrees well qualitatively with the analyses through late January when the stratopause was very low and ill-defined, and after early March when the stratopause had dropped/warmed. However, as expected given the proximity to the model tops and the lack of data constraints, the

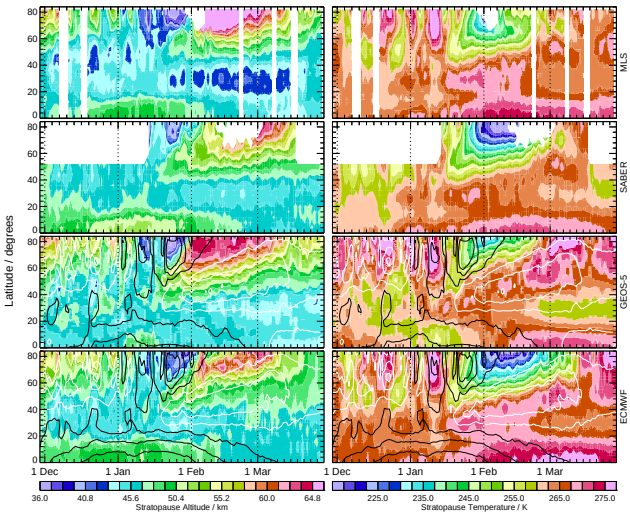

Figure 2. Latitude-time sections of (left) stratopause altitude (km, calculated using a "warm point" algorithm) and (right) stratopause temperature (K) from (top to bottom) MLS, SABER, GEOS-5 and ECMWF, from 1 December 2005 through 31 March 2006. Overlaid contours area as in Figure 1, but at 1 hPa.

analyses do not capture the reformation of the stratopause at high altitude; in fact, the level where it reforms is near or above the top analysis level. GEOS-4 and GEOS-5 show the stratopause reforming near 0.08 hPa with much higher temperatures than observed; the ECMWF stratopause remains cool and ill-defined until early March, and warms later than that in the satellite data. GEOS-4 and GEOS-5 show qualitatively similar evolution (Figure 1), but the polar stratopause in GEOS-4 is much too warm throughout the winter. When the stratopause is cold in late January and February, GEOS-5 temperatures are higher than in the satellite data and the cold region is confined nearer the pole; ECMWF shows lower temperatures for a longer time during this period. The qualitative differences between the analyses highlight the dependence on the underlying models and parameterizations.

Longitude-height sections at 70°N from satellite data and analyses (Figure 3), and maps of MLS stratopause altitude and temperature (Figure 4) detail the synoptic evolution of the stratopause. The analyses capture the structure of the stratopause before the peak of the SSW (Figure 3 and 4, 16 January). The stratopause is separated in longitude as well as latitude, with minimum altitude near 240°E, maximum altitude near 280°E, and lowest temperatures in the region between. The 16 January satellite data show a secondary temperature maximum extending up from the high altitude side, overlying the stratopause from ∼120 to 270°E; we have found this to be a common feature in the NH winter. Differences between the feature in MLS and SABER data are likely related largely to the poorer vertical resolution of MLS in the mesosphere [*Livesey et al.*, 2005]. This feature is too high to be captured by the analyses; both show a lower, less extended secondary maximum. The 30 January plots show dramatically how nearly isothermal the polar stratosphere is during the period after the SSW. Both MLS and SABER show weak local temperature maxima near 0.1 and 0.03 hPa. The GEOS-5 analysis shows a vertically-compressed version of the same pattern, whereas the ECMWF analysis shows a better representation of the lower part of the pattern, but no overlying second maximum. Cold and nearly isothermal conditions cover the entire polar region (Figure 4). On 25 February, when the stratopause has dropped and warmed towards typical values, the satellite data show the altitude varying smoothly around the latitude circle from about 0.01 to 0.68 hPa (Figures 3 and 4), with lowest temperatures in the transition regions between low and high stratopauses; the analyses capture the lower portion of this, but show the higher maxima at lower altitude, resulting in a much smaller range of stratopause altitudes.

Figure 5 shows the structure of the stratopause in relation to the stratospheric/mesospheric jet as a function of equivalent-latitude (EqL, the latitude that would enclose the same area as a given potential vorticity (PV) contour [*Butchart and Remsberg*, 1986]). The EqL/potential temperature sections of MLS temperature extend only as high as the GEOS-4 PV used for mapping is available, but avoid the smearing of values from different air masses inherent in zonal means. On 1 January, before the SSW (indicated by a strong jet throughout the stratosphere) the stratopause showed the characteristic separation [*Hitchman et al.*, 1989] across the upper part of the stratospheric polar vortex, but was slightly cooler than the mid-EqL stratopause. By 16 January, the vortex had broken down in the USLM (weak winds) and was rapidly weakening in the midstratosphere; the separated stratopause was still apparent, but it had dropped near the location of the weak jet, and warmed at highest EqLs. By 30 January, the polar stratopause was well below and much cooler than the mid-EqL stratopause; the polar vortex started to reform in the USLM, but with a lower latitude jet (larger vortex area). By 15 February, the vortex was very strong in the USLM, but only beginning to reform in the middle stratosphere (see also Figure 1). The stratopause was tilted upward along the jet axis, transitioning to being high and cold at highest EqLs.

3. Discussion and Summary

The evolution of the stratopause during the major stratospheric sudden warming (SSW) in January/February 2006

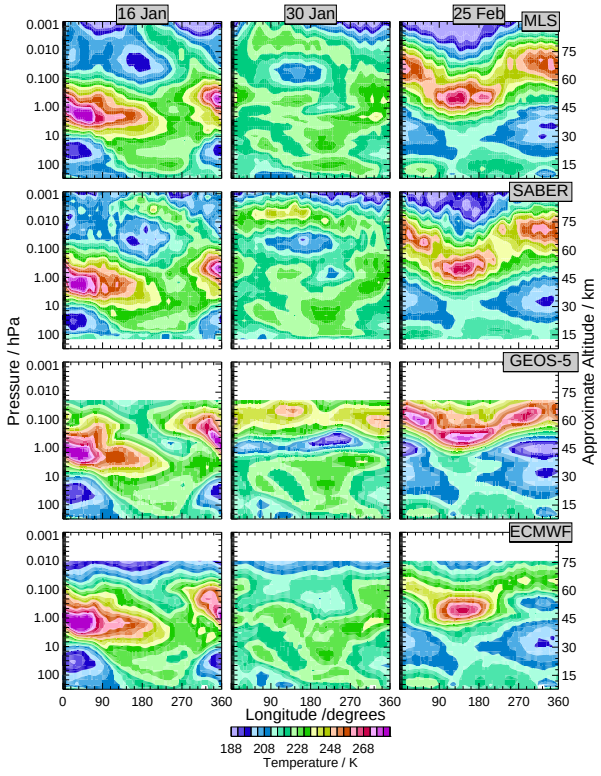

Figure 3. Longitude-pressure sections around 70°N of temperature (K) from (top to bottom) MLS, SABER, GEOS-5 and ECMWF, on (left to right) 16 and 30 January and 25 February 2006.

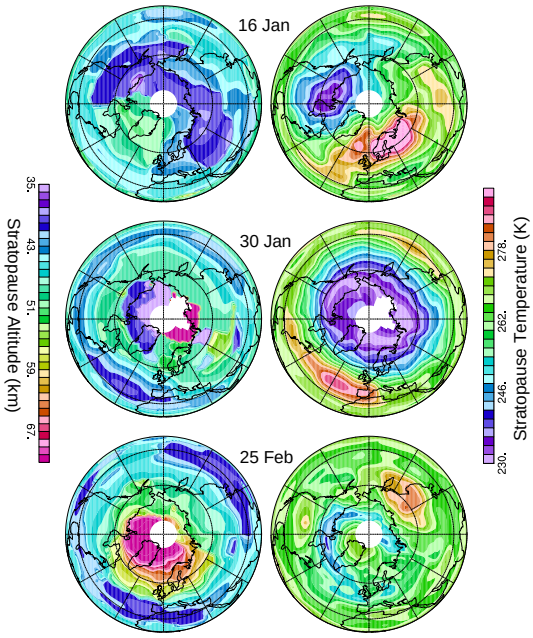

Figure 4. Maps of MLS stratopause altitude (km, left) and stratopause temperature (K, right) on 16 and 30 January and 25 February 2006. Projection is orthographic, with 0° longitude at the bottom and 90°E to the right; domain is 0 to 90°N.

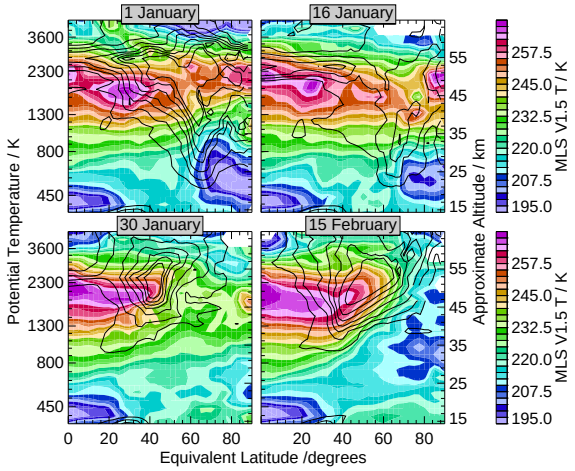

Figure 5. EqL/potential temperature sections of MLS temperature (K) on 1, 16, and 30 January and 15 February 2006. GEOS-4 EqL is used to map MLS data. Overlaid contours are GEOS-4 windspeeds from 30 to 90 m/s by 10 m/s.

has been detailed using MLS and SABER satellite data. The polar stratopause, initially higher than and separated from that in midlatitudes, dropped by 20–30 km during the SSW to near 30 km, warming during and then cooling after the peak of the SSW. After a period when the stratosphere was nearly isothermal, a cool polar stratopause reformed near 75 km, then rapidly warmed and dropped to near 55 km. The stratopause altitude during the SSW varied by over 40 km. The synoptic structure shows that the stratopause is separated in longitude as well as latitude, with lowest temperatures in the transition regions between higher and lower stratopauses.

Before and well after the warming, GEOS-4/5 and ECMWF meteorological analyses represent the structure and evolution well despite the lack of data constraint, with some quantitative differences. They do not, however, capture a commonly-seen secondary temperature maximum that overlies the stratopause. The analyses also cannot capture the very high stratopause after the SSW (which is near or above their top levels), the details of the nearly-isothermal region extending through the USLM, or the extent of altitude variations with longitude. They underestimate the extent of altitude variations during the SSW by 10-15 km. The inability of current analyses to capture the correct structure of the stratopause requires further investigation: Issues such as the double stratopause and the failure of the analyses to capture the high stratopause after the warming cast doubt on the adequacy of the GW drag codes for this task, either because of limitations in the codes themselves, the low upper boundaries of the underlying GCMs, or the remote impact of data insertion at lower levels. The results of *Siskind et al.* [2007] for a free-running GCM with a higher top suggest that more sophisticated GW parameterizations can improve the representation of these features. MLS and SABER provide the kind of high-quality, daily temperature observations covering the USLM that are needed to understand this region in detail and to improve its representation in models and assimilation systems.

The SSW in 2006 was unusually prolonged: The vortex reformed quickly and strongly in the upper stratosphere, but remained weak in the middle and lower stratosphere. This is very much like the pattern during the prolonged SSW in the 2003-2004 winter [*Manney et al.*, 2005]. SABER and GEOS-4 temperatures during the 2003-2004 warming show a very similar pattern of stratopause evolution to that in 2006. In contrast, a very brief major SSW in late February 2007, without a strong upper stratospheric recovery, produced only a very modest drop of the stratopause, with an immediate return to pre-SSW altitudes. Further study of stratopause evolution, both in existing and future satellite data and in the historical record using these comparisons as guidance for the types of behavior captured accurately by the analyses, can help elucidate the detailed mechanisms resulting in the observed behavior, and this improved understanding can help to model these events and explore possible implications for influence on the lower atmosphere and detection of climate effects.

Acknowledgments. We thank the MLS Science Team for their continuing support and assistance, NASA's GMAO for their GEOS-4/5 analyses, and the ECMWF for their T799L91 analyses. Research at the Jet Propulsion Laboratory, California Institute of Technology, is done under contract with the National Aeronautics and Space Administration.

References

Bloom, S. C., et al. (2005), The Goddard Earth Observing Data Assimilation System, GEOS DAS Version 4.0.3: Documentation and validation, *Tech. Rep. 104606 V26*, NASA.

Butchart, N., and E. E. Remsberg (1986), The area of the stratospheric polar vortex as a diagnostic for tracer transport on an isentropic surface, *J. Atmos. Sci.*, *43*, 1319–1339.

Froidevaux, L., et al. (2006), Early validation analyses of atmospheric profiles from EOS MLS on the Aura satellite, *IEEE Trans. Geosci. Remote Sens.*, *44*, 1106–1121.

Garcia, R. R., and B. A. Boville (1994), "Downward control" of the mean meridional circulation and temperature distribution of the polar winter stratosphere, *J. Atmos. Sci.*, *51*, 2238–2245.

Hitchman, M. H., J. C. Gille, C. D. Rodgers, and G. Brasseur (1989), The separated polar stratopause: A gravity wave driven climatological feature, *J. Atmos. Sci.*, *46*, 410–422.

Labitzke, K. (1972), Temperature changes in the mesosphere and stratosphere connected with circulation changes in winter, *J. Atmos. Sci.*, *29*, 756–766.

Livesey, N. J., et al. (2005), Version 1.5 level 2 data quality and description document, *Tech. Rep. JPL D-32381*, Jet Propulsion Laboratory.

Manney, G. L., K. Krüger, J. L. Sabutis, S. A. Sena, and S. Pawson (2005), The remarkable 2003-2004 winter and other recent warm winters in the Arctic stratosphere since the late 1990s, *J. Geophys. Res.*, *110*, D04,107, doi:10.1029/2004JD005,367.

Reinecker, M. M., et al. (2007), The GEOS-5 data assimilation system: A documentation of GEOS-5.0, *Tech. Rep. 104606 V27*, NASA.

Remsberg, E., et al. (2003), On the verification of the quality of SABER temperature, geopotential height, and wind fields by comparison with Met Office assimilated anylyses, *J. Geophys. Res.*, *108*, 4628, doi:10.1029/2003JD003,720.

Siskind, D. E., , S. D. Eckermann, L. Coy, and J. P. McCormack (2007), On recent interannual variability of the Arctic winter mesosphere: Implications for tracer descent, *Geophys. Res. Lett.*, in press.

Untch, A., M. Miller, M. Hortal, R. Buizza, and P. Janssen (2006), Towards a global meso-scale model: The high resolution system T799L91 and T399L62 EPS, *ECMWF Newsletter*, *108*, 6–13.

Waters, J. W., et al. (2006), The Earth Observing System Microwave Limb Sounder (EOS MLS) on the Aura satellite, *IEEE Trans. Geosci. Remote Sens.*, *44*, 1075–1092.

Gloria L. Manney, Mail Stop 183-701. Jet Propulsion Laboratory, California Institute of Technology, Pasadena, CA 91109, USA, Gloria.L.Manney@jpl.nasa.gov

This preprint was prepared with AGU's LaTeX macros v5.01, with the extension package 'AGU^{++}' by P. W. Daly, version 1.6b from 1999/08/19.